J Parasit Dis (Oct-Dec 2019) 43(4):658–671
https://doi.org/10.1007/s12639-019-01145-z

ORIGINAL ARTICLE

Evaluation of the therapeutic efficacy of albendazole-loaded silver nanoparticles against *Echinococcus granulosus* infection in experimental mice

Nashaat E. Nassef[1] · Abdel-Gawad E. Saad[2] · Nancy M. Harba[1] · Engy V. N. Beshay[1] · Marwa A. Gouda[2] · Sawsan S. Shendi[2] · Asmaa Shams El-Dein Mohamed[3]

Received: 20 March 2019 / Accepted: 10 July 2019 / Published online: 15 July 2019

Abstract The drug of choice for treatment of hydatid disease, albendazole (ABZ) is a poorly water-soluble drug; thus, enhancing its solubility is required. Among metal nanoparticles (NPs), silver (Ag) NPs showed antimicrobial efficacies. Therefore, this study was conducted to evaluate nanosilver particles (Ag NPs) free or combined with albendazole against *Echinococcus granulosus* infection in vivo. In this study, besides the normal control group (GI) (n = 5), 80 mice were infected with 2000 viable protoscoleces intraperitoneally then divided equally (n = 20) into the infected control (GII), ABZ-treated (GIII), nanosilver-treated (GIV) and ABZ-loaded-Ag NPs-treated (GV) groups. On the 90th post-infection day, treatment was started and continued for 8 weeks then the experiment was terminated. Each mouse was subjected to measurement of hydatid cysts' sizes and weights, serum IFN-γ, liver enzymes; histopathological and transmission electron microscopy studies. In all treated groups, there were significant reductions of hydatid cysts' sizes and weights; however, the highest efficacy rate (63.9%) was detected in group V associated with obvious ultrastructure alterations of the cysts. The liver tissues of group II showed intense granulomatous reactions, congestion, fibrosis, necrosis and steatosis associated with significant increases in serum IFN-γ and liver enzymes. Interestingly, the best antiparasitic effect and the most significant reduction of IFN-γ towards the normal values were found in GV. Moreover, Ag NPs had reduced the toxic effects of ABZ such as necrosis, steatosis and the elevated serum liver enzymes. Therefore, loading ABZ on Ag NPs could be a potential method to improve ABZ efficacy against hydatid disease.

Keywords Albendazole · *E. granulosus* · IFN-γ · In vivo · Nanosilver particles · Ultrastructure

Introduction

Cystic echinococcosis (CE) is a worldwide zoonotic parasitic disease caused by the larval stages of dog tapeworm *Echinococcus granulosus* (Moro and Schantz 2009). The disease is endemic in the Middle East, North Africa, the Mediterranean region and Egypt (Kandeel et al. 2004).

Human infection with *E. granulosus* eggs results in the development of one or multiple unilocular hydatid cysts. The cyst is spherical, fluid-filled sac consisting of an inner cellular germinal layer supported by an acellular laminated layer. It becomes enclosed by a host granulomatous reaction followed by the development of a fibrous layer (Moro and Schantz 2009). The cysts develop mostly in the liver (70%), lungs (20%) and 10% of cysts may take place anywhere in the body. The cysts are slowly growing and tolerable until they reach the sizes which lead to malfunction of the affected organ (Grosso et al. 2012).

Depending on cyst number, size and site, there are four treatment lines for CE: surgical removal, percutaneous aspiration injection respiration (PAIR) procedures, chemotherapy or watch and wait (Stojkovic et al. 2009).

✉ Engy V. N. Beshay
engy.victor77@yahoo.com;
engyvictor@med.menofia.edu.eg

[1] Medical Parasitology Department, Faculty of Medicine, Menoufia University, Yassin abdel Gaffar St. from Gamal Abdel Nasser St., Shebin El-Kom, Menoufia, Egypt

[2] Clinical and Molecular Parasitology Department, National Liver Institute, Menoufia University, Shebin El-Kom, Egypt

[3] Pathology Department, Faculty of Medicine, Menoufia University, Shebin El-Kom, Egypt

When the cysts are in multiple organs or at inaccessible sites, the invasive methods become unfeasible and the chemotherapy remains to be the only choice (Higuita et al. 2016).

The commonly used drugs for treatment of hydatid cyst are mebendazole and albendazole (ABZ) (McManus et al. 2012). However, therapeutic failures with ABZ were reported and have been linked to its low water solubility, poor gastrointestinal absorption and low drug concentrations in plasma and hydatid cysts fluid (Jelowdar et al. 2017). Thus, changing the physical properties of the drug seems to be a possible way to overcome this problem (Pensel et al. 2018).

Enhancing aqueous solubility and bioavailability of poor soluble drugs has been achieved by loading these drugs with nanoparticles (NPs) owing to the various unique properties of NPs such as their large surface-volume ratio and their high ability to enter inside the cells (Horton 2018). Among several metal NPs, the synthesized silver NPs (Ag-NPs) was found a nontoxic substance with satisfactory antimicrobial efficacies against viruses, bacteria and parasites. Moreover, it was evaluated as a suitable carrier of various therapeutic drugs (Burduşel et al. 2018). Therefore, this study was designed to evaluate the therapeutic effects of silver nanoparticles alone and combined with albendazole against *E. granulosus* infection in an experimental mice model. The therapeutic effects were assessed through parasitological, histopathological, transmission electron microscopy (TEM) studies. Additionally, serological assessment of IFN-γ in mice sera by ELISA and measurement of liver enzymes were done.

Materials and methods

Parasite

Hydatid cysts were obtained from El-Warrak slaughter house in Cairo, Egypt. The protoscoleces were prepared according to Amri et al. (2007). Briefly, the hydatid fluid was aspirated from fertile cattle pulmonary cysts under aseptic conditions. The fluid was centrifuged and the sediment containing PSCs was washed with sterile phosphate buffer saline (PBS) supplemented with 30 mg/mL gentamicin. The viability of PSCs was assessed by their movement observed under an inverted microscope after staining by 0.1% eosin. The unstained and moving PSCs were counted as viable. A percentage of viable PSCs of more than 95% was considered suitable for further experimental infection. For each mouse, the infective inoculum was adjusted to contain 2000 viable PSCs suspended in 500 µL of sterile PBS for intraperitoneal inoculation (Urrea-Paris et al. 2002).

Tested drugs

Albendazole suspension (ABZ) (Albendazole® 400 mg/10 mL; Pharma Cure Pharmaceuticals Co., Cairo, Egypt) was dissolved in 0.2 mL chromphore L and given orally via a gastric tube at a dose of 200 mg/kg/d for 5 consecutive days per week for 8 weeks (Küster et al. 2014). Nanosilver particles reagents of chemical trade were purchased from Sigma-Aldrich Chemical Company. Silver NPs were synthesized by chemical reduction method according to Solomon et al. (2007). Conversion of the brownish yellow color of the reagents into dark brown color indicated the synthesis of silver nanoparticles. Characterization of the nanoparticles was done as described by Liang et al. (2018). The average size of the prepared AgNPs was around 100 nm. Mice were given silver nanoparticles orally via a gastric tube at a dose of 25 mg/kg/d dissolved in 0.2 mL of chromphore L for 2 months (Shanmugasundaram et al. 2017). The in vivo toxicity of AgNPs was examined previously by Shanmugasundaram et al. (2017) and they determined the No-Observed-Adverse-Effect-Level (NOAEL) of the Ag-NPs was 2000 mg/kg bw. Moreover, the possible toxicity of AgNPs was avoided by using the minimum effective dose against hepatocellular carcinoma in a mouse model which was used by the same authors. Albendazole-loaded nanoparticles were prepared as described by Noorani et al. (2015). Drug loading efficacy and encapsulation efficacy were calculated according to the following equations:

$$Loading\ efficacy = \frac{C\,abz - V}{Mn} \times 100\%$$

$$Encapsulation\ efficacy = \frac{C\,abz - V}{M\,abz} \times 100\%$$

where *C abz* is the concentration of ABZ (mg/mL), *V* is volume of the solution (mL), *Mn* is the weight of the total silver nanoparticles (mg) and *M abz* is the total weight of ABZ (mg).

Mice were given ABZ-loaded on silver nanoparticles orally via a gastric tube at a dose of 100 mg/kg/d dissolved in 0.2 mL of chromphore L for 8 weeks.

Experimental animals

Pathogen-free laboratory-bred female albino mice, 6–8 weeks of age and weighing 24 ± 2 g were purchased from the Biology Supply Center at Theodor Bilharz Research Institute (PO Box 30 Imbaba, Giza, Egypt). Mice were housed under a controlled room temperature (22 ± 1 °C) with free access to the standard pellet animal diet and water. The study was approved by the Scientific Research Ethical Committee, Faculty of Medicine, Menoufia University. Also, animal handling and all

procedures were done in accordance with the international ethical guidelines.

Experimental design

In this study, 85 mice were used; five healthy non-infected mice were assigned to the normal control group (GI) and 80 *E. granulosus*-infected mice were divided randomly into the following four groups each of 20 mice (n = 20): Group II was the infected untreated group (positive control); Group III was treated with albendazole. Group IV was treated with silver nanoparticles and Group V was treated with albendazole loaded on silver nanoparticles. All treatment regimens were started on 90th day post infection (p.i.) and continued for 8 weeks and 1 week after administration of the last doses of the tested drugs, the experiment was terminated.

At the end of the study, each mouse was anaesthetized with ether, blood sampling via a cardiac puncture and the sacrifice by cervical dislocation were performed. Blood samples were centrifuged and sera were separated and stored at − 80 °C for further serological and biochemical studies. Each mouse was subjected to measuring hydatid cyst size and weight followed by a TEM study; histopathological examination of the liver tissue then measurement of serum IFN-γ and liver enzymes.

Hydatid cyst size, weight and treatment efficacies

At necropsy of each mouse, the peritoneal cavity was opened carefully and different organs were inspected. The hydatid cysts were photographed by a digital still camera and the sizes of the cysts were determined by the scaled ruler using Adobe Photoshop CS3. The cysts were carefully removed and the weight was determined using an analytical balance. The efficacy rate of treatments was calculated by the use of the following formula (Pensel et al. 2015).

$$Treatment\ efficacy = \frac{C - T}{C} \times 100\%$$

where C is the mean cyst weight or size in the infected non treated control group and T is the mean cyst weight or size in the treated group.

Histopathological study

From each animal, liver tissue samples were fixed in 10% formalin, embedded in paraffin and processed into blocks. Serial sections of 5 μm in thickness were cut then stained with hematoxylin and eosin (Drury and Wallington 1980). The sections were examined under a light microscope (Olympus BX41, Olympus Corporation, Tokyo, Japan).

Transmission electron microscopy (TEM)

For ultrastructure examination of the retrieved hydatid cysts, the samples were processed as previously described (Elissondo et al. 2006). The samples were photographed at the Faculty of Agriculture, Cairo University. With a JEOL JEM 1230 transmission electron microscope (JEOL, Tokyo, Japan) operated at an accelerating voltage of 80 kV.

Measurement of IFN-γ in mice serum samples

Detection of IFN-γ in mice serum samples was done by sandwich Enzyme linked immunosorbent assay (ELISA) (Quantikine® R&D systems, Inc. Minneapolis, USA). Serum samples were tested according to the manufacturer's instructions and the amounts of IFN-γ were expressed as pg/mL.

Biochemical assays of liver enzymes

Alanine transeferase enzyme (ALT), Aspartate transeferase enzyme (AST) and Alkaline phosphatase enzyme (ALP) activities were measured according to manufacturer's instructions of the assay kits (Adicon Clinical Laboratories, Shanghai, China) and the enzymes' activities were expressed as U/L.

Statistical analysis

The data were collected, tabulated and analyzed by statistical package for the social science software version 20 (SPSS, IBM, Armonk, USA). The descriptive data were expressed as percentages and examined by Chi square test. The numerical data were expressed as mean ± standard deviation (SD). The data were tested for normality using the Kolmogorov–Smirnov test. To test the significance of nonparametric data, Kruskal–Wallis test was applied and followed by a post hoc test to determine the significance of data between the different groups. Results with $P \leq 0.05$ were considered significant.

Results

Mortality rate

Regarding the mortality rate among different studied groups, there was no significant difference between the studied groups ($P > 0.05$). However, the highest mortality rate was reported in the infected control group (GII) as six (30%) mice died. While each treated group showed a rate of 15% due to death of three mice.

Table 1 Comparison of hydatid cyst size and weight among the different studied groups

	The studied groups				Kruskal–Wallis test	*P* value	Significant post hoc
	GII (infected control) (n = 14)	GIII (ALZ) (n = 17)	GIV (nanosilver particles) (n = 17)	GV (ALZ-loaded nanoparticles) (n = 17)			
Hydatid cyst size (mm)							P1 = 0.0001
Mean ± SD	5.14 ± 1.75	1.25 ± 0.85	0.57 ± 0.43	0.39 ± 0.48	52.324	0.0001	P2 = 0.0001
Median (minimum–maximum)	6 (3–7)	1.70 (0–2)	0.80 (0–1)	0.00 (0–1)			P3 = 0.0001
							P4 = 0.02
Hydatid cyst weight (g)							P1 = 0.003
Mean ± SD	0.78 ± 0.08	0.43 ± 0.29	0.18 ± 0.15	0.11 ± 0.14	46.325	0.001	P2 = 0.0001
Median (minimum–maximum)	0.8 (0.7–0.9)	0.6 (0.0–0.7)	0.2 (0.0–0.4)	0.0 (0.0–0.3)			P3 = 0.0001
							P4 = 0.008
Treatment efficacy %	–	22.9	54.9	63.9			

P1 = GIII (ABZ) versus GII (positive control)

P2 = GIV (nanosilver particles) versus GII (positive control)

P3 = GV (ABZ-loaded nanoparticles) versus GII (positive control)

P4 = GV (ABZ-loaded nanoparticles) versus GIII (ABZ)

Hydatid cyst sizes, weights and efficacy rates of treatments

Regarding hydatid cyst sizes and weight, there was a significant difference ($P < 0.001$) between infected treated groups (GIII, GIV and GV) when they were compared with the infected control group (GII). The biggest hydatid cyst size and weight (5.14 ± 1.75 mm, 0.78 ± 0.08 g) were detected in the infected control group (GII). All the treated groups showed significant reductions; however, the smallest values were detected in ABZ-loaded nanoparticles-treated group (GV). Accordingly, the treatment efficacy of ABZ was 22.9% while the efficacy of nanosilver treatment was 54.9%. The highest efficacy rate (63.9%) was obtained with ABZ-loaded nanoparticles (Table 1).

Histopathological results

Regarding the granuloma size, there was a significant difference between the treated groups (GIII, GIV and GV) and the infected control group (GII) ($P < 0.05$). The largest size was reported in GII (9.36 ± 1.81) and the smallest granuloma size (0.47 ± 0.51 mm) was detected in ABZ-loaded nanoparticles-treated group (GV) (Fig. 4) (Table 2).

Concerning fibrosis (Fig. 5a) and inflammatory infiltration of liver tissues (Fig. 5b), there were significant

Table 2 Comparison of granuloma size among the different studied groups

Granuloma size (mm)	The studied groups				Kruskal–Wallis test	*P* value	Significant post hoc
	GII (Positive control) (n = 14)	GIII (ABZ) (n = 17)	GIV (nanosilver particles) (n = 17)	GV (ABZ-loaded nanoparticles) (n = 17)			
Mean ± SD	9.36 ± 1.81	3.00 ± 1.21	3.06 ± 1.22	0.47 ± 0.51	138.69	0.000	P1 = 0.0001
Median	8 (6–10)	2 (1–4)	2 (1–4)	0.00 (0–1)			P2 = 0.0001
							P3 = 0.0001
							P4 = 0.0001
							P5 = 0.0001

P1 = GIII (ABZ) versus GII (positive control)

P2 = GIV (nanosilver particles) versus GII (positive control)

P3 = GV (ABZ-loaded nanoparticles) versus GII (positive control)

P4 = GV (ABZ-loaded nanoparticles) versus GIII (ABZ)

P5 = GV (ABZ-loaded nanoparticles) versus GIII

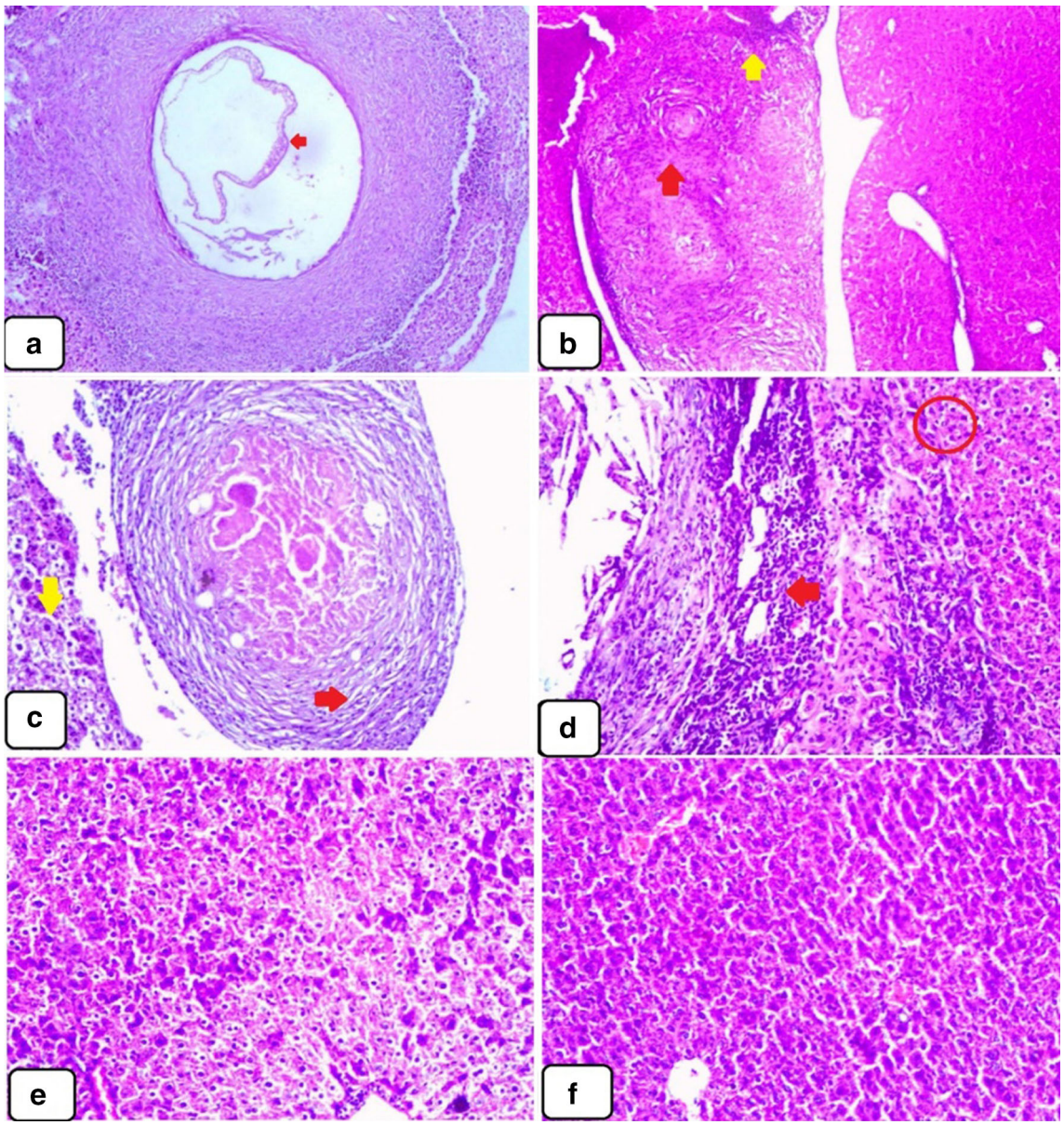

Fig. 1 Haematoxylin and eosin stained liver sections from *E. granulosus*-infected control group (GII). **a** Showing a hydatid cyst with an intact germinal layer (red arrow) and a laminated layer. The cyst is surrounded by granulomatous reaction with dense fibrosis and inflammatory infiltrate (×40). **b** Showing a granulomatous reaction (red arrow) with moderate infiltration by chronic inflammatory cells (lymphocytes) (green arrow) (×40). **c** Showing granulomatous lesion with thick fibrotic wall (red arrow) and the surrounding liver parenchyma shows severe parenchymal damage (yellow arrow) (×100). **d** Showing a granulomatous reaction with a dense collection of lymphocytes (red arrow) and the surrounding liver parenchyma shows focal cellular degeneration (red circle) (×100). **e** Showing diffuse apoptosis and necrosis (×100). **f** Showing apoptosis and congestion of sinusoids (×100) (color figure online)

differences between the treated groups (GIII, GIV and GV) and the infected control group (GII) ($P < 0.05$). In the infected control group (GII), 71.4% and 57.1% showed severe fibrosis and inflammatory infiltration (infiltration and focal aggregations of lymphocytes and macrophages in portal areas and in hepatic parenchyma), respectively (Fig. 1). Obvious improvements were observed in ABZ-treated (GIII) (Fig. 2) and nanosilver-treated (GIV) groups (Fig. 3). However, the best results were detected in ABZ-loaded nanoparticles-treated group (GV) (Fig. 4).

As regards liver cell necrosis (Fig. 5c) and steatosis (hepatocyte cytoplasm is occupied by a single large lipid vacuole), (Fig. 5d), there was a significant difference between the studied groups ($P = 0.000$). Interestingly, the ABZ-treated group (GII) (Fig. 2), showed the highest values of liver cell necrosis and steatosis. Noticeable

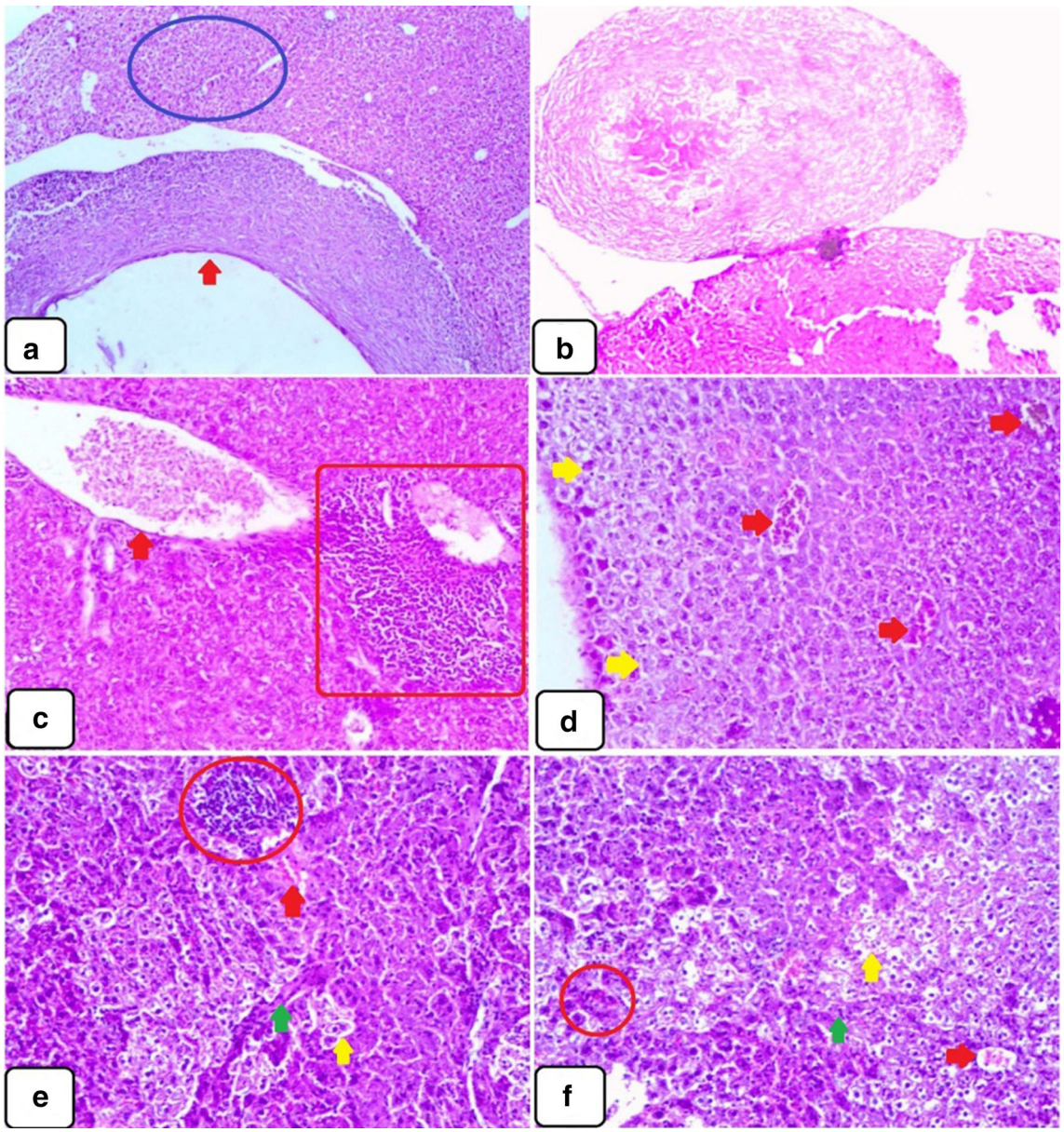

Fig. 2 Haematoxylin and eosin stained liver sections from *E. granulosus*-infected ABZ-treated group (GIII). **a** Showing a hydatid cyst (red arrow) germinal layer and laminated layer. The cyst is surrounded by moderate granulomatous reaction, fibrosis and inflammatory infiltrate. Liver parenchyma shows areas of degeneration and necrosis (blue circle) (×200). **b** Showing a granulomatous reaction with moderate fibrosis (×40). **c** Showing markedly congested central veins and hepatic sinusoids (red arrow) with dense collection of lymphocytes at the portal tract (red rectangle) (×100). **d** Showing markedly congested central veins and hepatic sinusoids (red arrows) with scattered cellular degeneration (yellow arrows) (×100). **e**, **f** Showing marked damage of liver parenchyma with frequent cellular apoptosis, moderate infiltration by inflammatory cells (red circle), congested sinusoids (red arrow), areas of necrosis and steatosis (yellow arrow) and fibrosis (green arrow) (×100) (color figure online)

improvements were observed in ABZ loaded nanoparticles-treated group (GV) (Fig. 4). However, the best results were detected in nanosilver-treated group (GIV) (Fig. 3).

Transmission electron microscopy

The ultrastructure of the hydatid cysts obtained from GII revealed intact germinal layer with microtriches projecting into the laminated layer. Undifferentiated cells with intact nuclear membranes and non-distorted nucleus were also seen. The cytoplasm of these cells was intact and rich in glycogen granules (Fig. 6a, b). The hydatid cysts from the ABZ-treated group (GIII) showed slightly vacuolated cytoplasm, glycogen depletion and heterochromatin (pyknosis) in the nucleus (Fig. 6c, d). The hydatid cysts retrieved from the nanosilver and ABZ-nanoparticle-

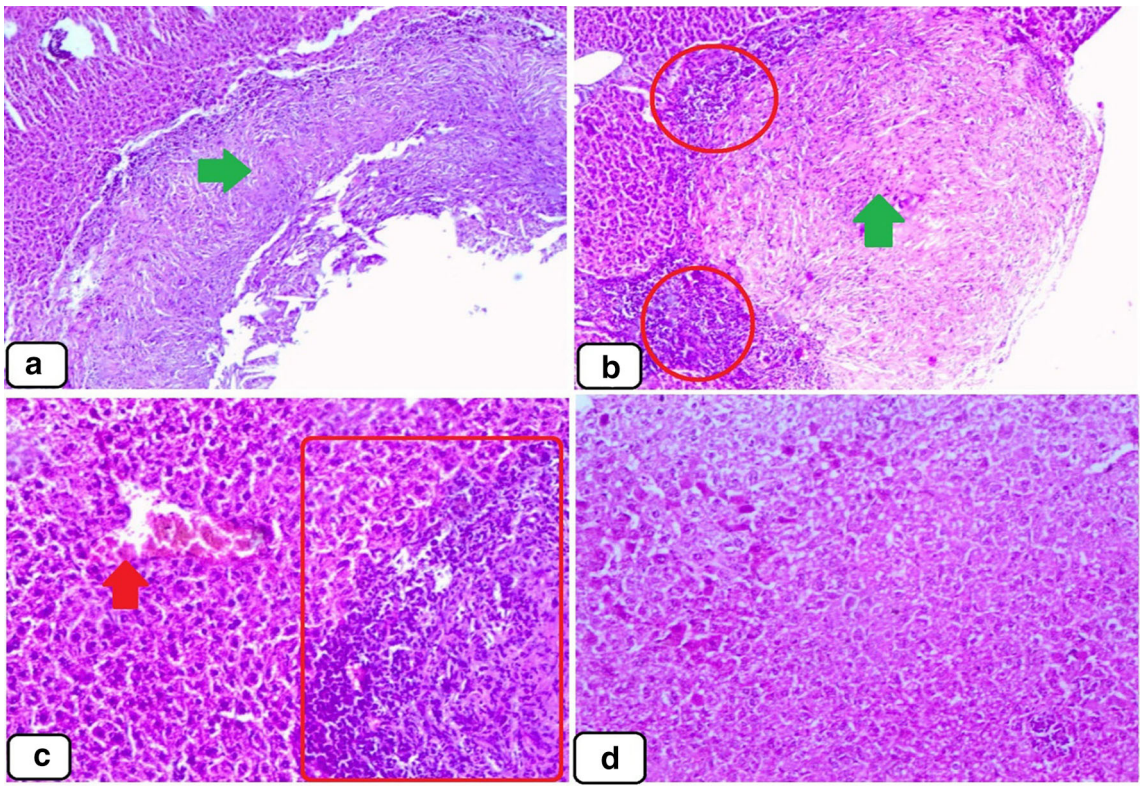

Fig. 3 Haematoxylin and eosin stained liver sections from *E. granulosus*-infected Ag NPs-treated group (GIV). **a** Showing a damaged hydatid cyst surrounded by moderate granulomatous reaction, fibrosis and inflammatory infiltrate (green arrow) (×40). **b** Showing a granulomatous reaction with moderate fibrosis with moderate inflammatory infiltrate in the form of scattered lymphocytic collections (×40). **c** Showing granulomatous lesion with moderate lymphocytic collection and fibrosis (red rectangle). The surrounding liver parenchyma shows a congested sinusoid (red arrow) with scattered cellular apoptosis (×100). **d** Showing scattered liver cellular necrosis and mild inflammatory infiltrate (×100) (color figure online)

treated (GV) groups showed destruction of the germinal layer with the loss of microtriches, separation from the laminated layer and depletion of glycogen. The nanosilver particles appeared as black rods inside the nuclei which showed fragmentations. The cytoplasm showed distortion of the mitochondria, glycogen depletion and autophagosomes in vacuolated cytoplasm. However, these changes were more obvious with ABZ-loaded nanoparticles (Fig. 7).

Serum values of IFN-γ

There was a significant difference ($P = 0.0001$) between the studied groups. There were significant increases in the serum IFN-γ in all groups when compared with the normal control group (GI). The highest significant increase was in ABZ-treated group when compared with GI and GII. Interestingly, with nanosilver treatment either alone (GIV) or combined with ABZ (GV), there were significant reductions in serum IFN-γ when they were compared with the infected control (GII) and ABZ-treated (GIII) groups. Moreover, the most significant decrease was in ABZ-loaded nanoparticles-treated group (GV). However these significant reductions, the values did not reach the normal values (Fig. 8).

Liver enzymes

There were significant increases ($P < 0.001$) of the serum levels of ALT, AST in the infected control group (GII) in comparison with the normal control group (GI). In ABZ-treated group (GIII), there were increases in the levels of ALT, AST and ALP when they were compared with GI; however, the differences were not significant except for ALP ($P = 0.03$). An obvious improvement of liver enzymes was found only in the ABZ-loaded Ag NPs-treated group (GV) when it was compared with the infected control (GII); but, this improvement was not significant and the values were still significantly higher than the normal control group (GI) ($P = 0.000$) (Fig. 9).

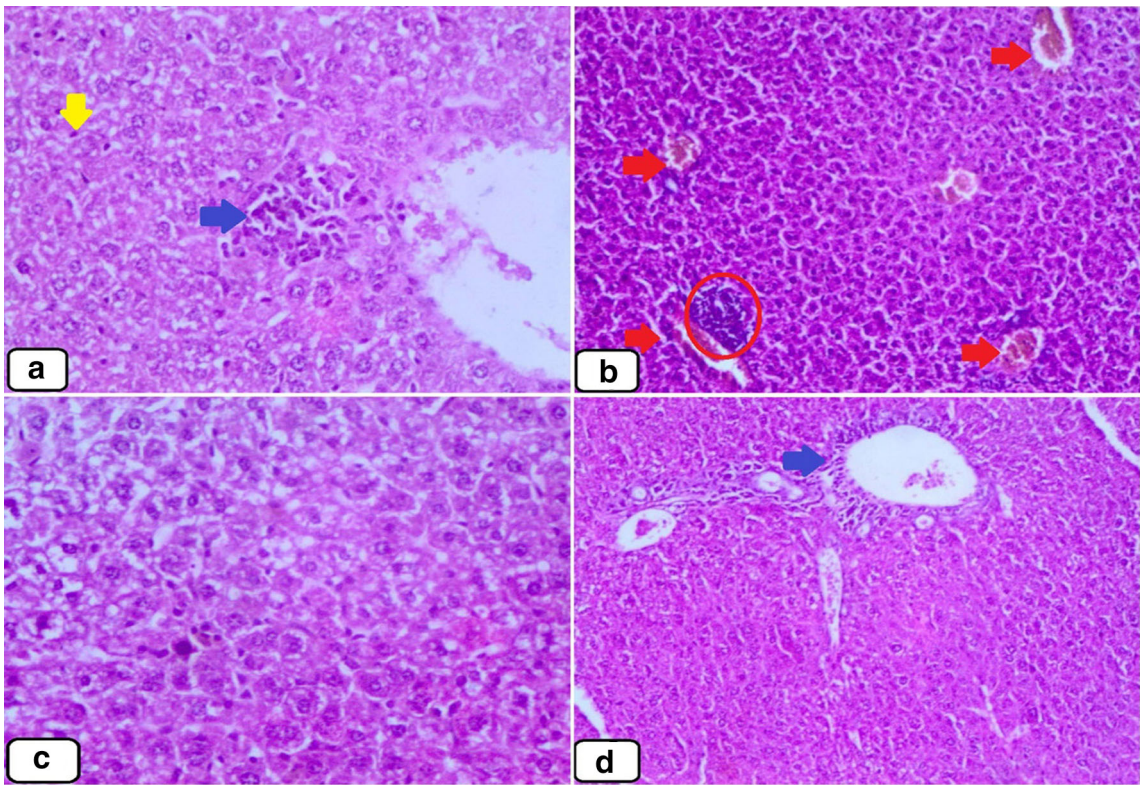

Fig. 4 Haematoxylin and eosin stained liver sections from *E. granulosus*-infected ABZ-loaded with Ag NPs-treated group (GV). **a** Showing scattered collections of lymphocytes (blue arrow). The liver parenchyma showed scattered degenerated necrotic cells (yellow arrow) (×200). **b** Showing mild congestion of the central vein (red arrows) with mild inflammatory infiltrate (red circle) (×100). **c** Showing area with steatosis and apoptosis (×200). **d** Showing scattered inflammatory infiltrate (blue arrow). Notably, there is no fibrosis, congestion, necrosis or steatosis (×100) (color figure online)

Discussion

Hydatid disease is a severe, neglected and an endemic parasitic disease in many countries (Nunnari et al. 2012). However the availability of chemotherapeutic drugs for this disease, they still need improvement (Luo et al. 2018). For example, the current drug of choice albendazole is a poor water-soluble drug; thus, enhancing its aqueous solubility is required (Horton 2018). Fortunately, this could be achieved by loading drugs with nanoparticles which have been widely used and satisfactory results were obtained (Farhadi et al. 2018).

Silver NPs (Ag-NPs) is a nontoxic substance with satisfactory antimicrobial efficacy against viruses, bacteria and parasites (Burduşel et al. 2018) and it showed a scolicidal effect in vitro (Rahimi et al. 2015). However, to the best of our knowledge, there is no previous study conducted to evaluate its efficacy in vivo. Therefore, this study was designed to evaluate the therapeutic effects of silver nanoparticles alone and combined with albendazole against *E. granulosus* infection in experimental mice.

The results of the present study revealed significant reductions of hydatid cysts' sizes and weights in all the treated groups; however, the smallest values with the highest efficacy rate (63.9%) were detected in ABZ-loaded nanoparticles-treated group (GV). Therefore, silver nanoparticles showed antiparasitic effect against *E. granulosus* infection in experimental mice and ABZ-loaded on nanoparticles was found more effective than the free drugs. These results correlated with the results obtained by our TEM study which revealed the occurrence of morphological alterations in all the cysts obtained from all the treated groups; however, those retrieved from ABZ-loaded nanoparticles-treated group showed the most noticeable changes (Figs. 5, 6).

Regarding TEM results obtained with albendazole in this study, similar results were reported by Wang et al. (2017). Our results could be attributed to the inhibition of polymerization of cytoskeletal tubulin, which results in suppression of cell division and disruption of secretory transport systems that end in necrosis vacuolation of the tegumental layer and death of the parasite (Palomares et al. 2006). Moreover, ABZ is known to inhibit glucose absorption by the parasite leading to glycogen depletion and degenerative changes in the parasite (Nunnari et al. 2012).

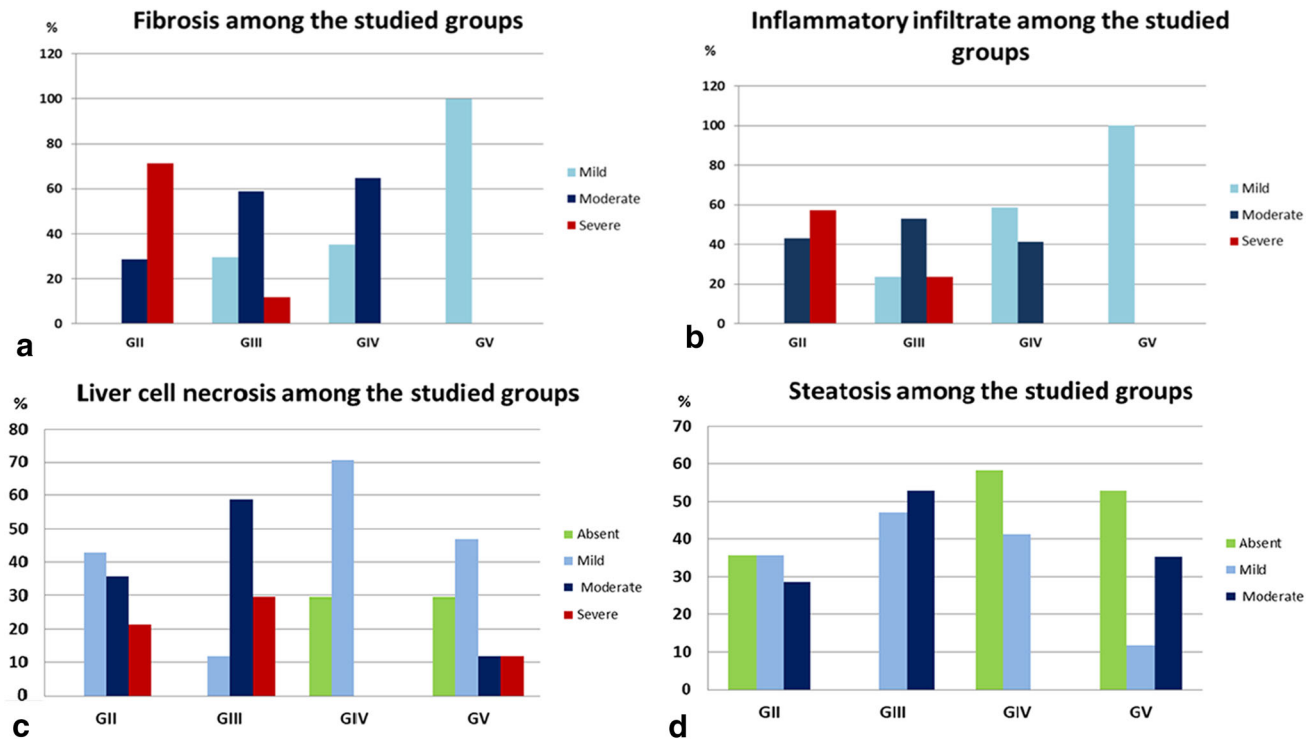

Fig. 5 Histopathological findings in the different studied groups. Data are expressed as percentages and examined for significance by Fisher exact test. **a**, **b** Showing significant improvement of fibrosis (Chi square = 59.531, $P = 0.000$) and inflammatory infiltrate (Chi square = 45.003, $P = 0.000$) in all treated groups, respectively; however, the best results were obtained in GV (ABZ-loaded Ag NPs-treated group). **c**, **d** Showing significant ($P = 0.000$) difference between groups regarding liver cell necrosis and steatosis, respectively. ABZ treatment (GIII) resulted in obvious increase in necrosis (Chi square = 207.266, $P = 0.000$) and steatosis (Chi square = 127.447, $P = 0.000$), the combined treatment (GV) resulted in improvement of both parameters while the best results are in nanosilver-treated group (GIV)

In this study, ABZ showed treatment efficacy of 22.9%. This result is in harmony with Moro and Schantz (2009) who stated that about 30–50% of patients may show a therapeutic response while 20–40% of patients with CE do not respond to ABZ therapy which is linked to the poor water solubility of ABZ which reduces its bioavailability and absorption from the intestinal tract (Horton 2018).

On contrary, ABZ efficacy in this study was lower than that obtained with Pensel et al. (2015) who reported 46.9% efficacy of ABZ against CE in experimental mice. This difference could be attributed to the different ABZ formulations used, as they used albendazole sulphoxide which is an active metabolite of ABZ that achieves high concentrations inside the cyst (Elissondo et al. 2013).

Concerning the mechanism of action of silver NPs, they have been reported to interact with the cell membrane and lead to the formation of pores and leakage of cellular contents. Moreover, they increase reactive oxygen species (ROS) formation which damages the mitochondrial membranes that finally leads to the initiation of programmed cell death "apoptosis" (Rai et al. 2017). Accordingly, the combination of ABZ and silver NPs can inhibit tubulin polymerization, glycolysis and mitochondrial functions. Moreover, the results obtained in our study could be linked to the enhanced dispersion of ABZ from the nanoparticles across the hydatid cyst layers (Jelowdar et al. 2017; Soltani et al. 2017). This dispersion was proved through our TEM study which revealed that silver nanoparticles had entered inside the cells, stimulated apoptosis, and autophagy and induced marked damage of hydatid cysts (Fig. 7). Interestingly in a similar way of action, Liang et al. (2018) found ABZ-Ag-NPs combination was effective against tumour cells both in vitro and in vivo.

The results of the present study are in consistency with several studies which have shown the efficacy of ABZ-loaded on nanoparticles against hydatid disease in experimental animals. For example, Ahmadnia et al. (2013) found that treatment of mice with albendazole sulfoxide and albendazole sulfoxide-loaded solid lipid nanoparticles (SLN) resulted in the reduction of the cysts' weights when they were compared to the control groups; however, these reductions were not statistically significant. Also, Liang et al. (2014) found a significant reduction of hydatid cysts weight with albendazole-loaded with chitosan. Similarly,

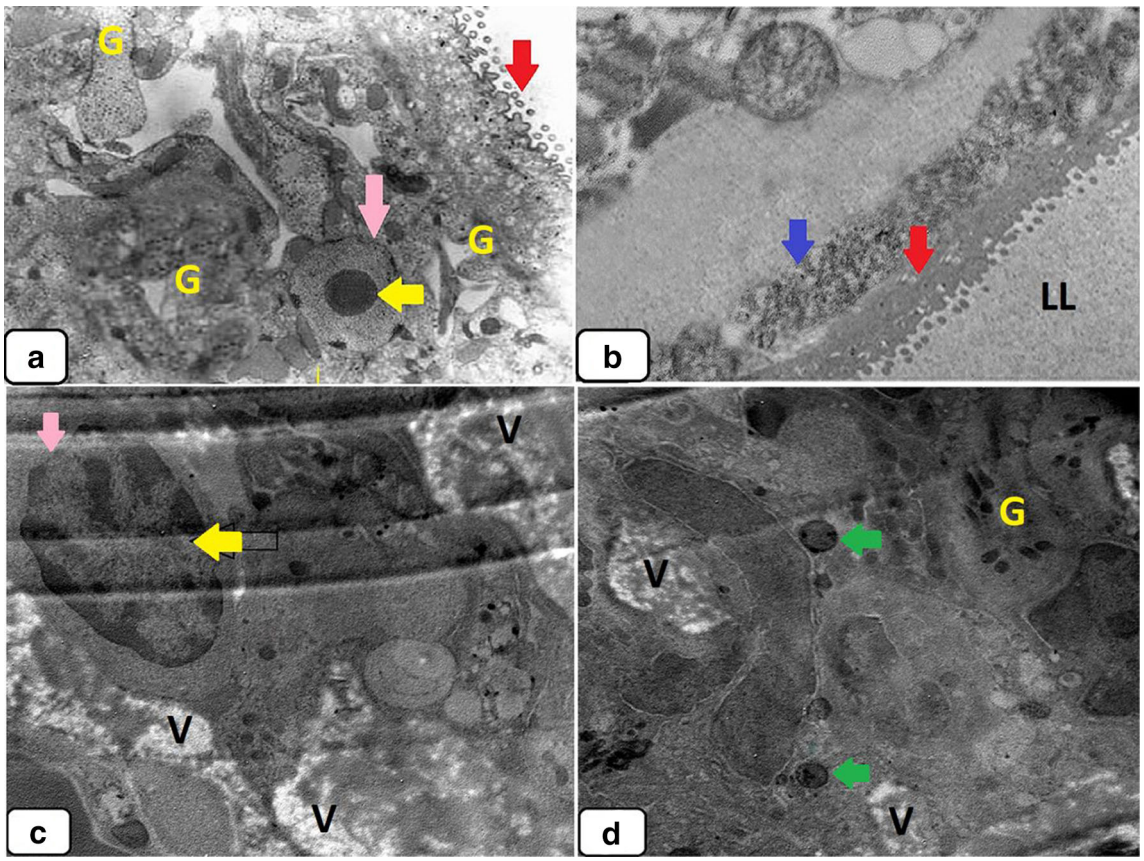

Fig. 6 Transmission electron micrograph of hydatid cysts **a**, **b** from an infected non treated mouse (GII) showing intact germinal layer with microtriches (red arrow) projecting into the laminated layer (LL) and distal cytoplasm (blue arrow). The germinal layer shows intact non differentiated cells with intact nuclear membrane (pink arrow), nucleus and nucleolus (yellow arrow). The cytoplasm is intact and rich in electron dense glycogen granules (×10,000). **c**, **d** TEM micrograph of hydatid cysts from ABZ-treated group (GIII) showing vacuolated cytoplasm (V), glycogen (G) depletion and autophagolysosomes (green arrow) and heterochromatin (pyknosis) in the nucleus (yellow arrow) with intact nuclear membrane (pink arrow) (×10,000) (color figure online)

Jelowdar et al. (2017) demonstrated that ABZ and PZQ-loaded with SLN were better than free ABZ or PZQ for the chemoprophylaxis of CE in mice. Recently, Farhadi et al. (2018) found that the weight of the cysts in flubendazole-loaded nanoparticles-treated group was significantly lower than those of the control and the free flubendazole-treated groups.

Our histopathological study revealed the occurrence of granulomatous reactions in association with liver congestion, haemorrhage, fibrosis, liver cell necrosis, degenerative changes and steatosis mainly in the infected control group and to some extent in the treated groups. These results are similar to the histopathological picture of the liver of experimentally infected mice (Al-Kuraishi 2009) and naturally infected sheep (Beigh et al. 2017).

In fact, the hydatid cyst stimulates a host's inflammatory reaction that ends in the formation of a fibrous capsule (Solcan et al. 2010), and the areas in between cysts usually show congestion, haemorrhage, liver cell necrosis together with fibrosis and inflammatory infiltration (Singh et al. 2014) with dilatation of the sinusoids and the central veins (Beigh et al. 2017).

In the present work, the results revealed improvements of the granuloma sizes, fibrosis, congestion and the inflammatory infiltrates in all the treated groups. However, free nanosilver was slightly better than free ABZ and the best results were obtained with ABZ-loaded nanosilver treatment. Moreover, liver cell necrosis and steatosis were increased with free ABZ treatment denoting a hepatotoxic effect of this drug. Conversely, improvements were observed with nanosilver treatments indicating the potential safety of AgNPs in vivo. In the same context, the highest serum levels of ALT, AST and ALP were found with ABZ treatment when they were compared with normal control group and the infection control group. On the other hand, improvements in liver enzymes were recorded in ABZ-loaded with Ag NPs-treated group (GIV).

The hepatotoxic effect of albendazle was documented before and it is known to be one of the drugs that may cause acute hepatitis characterized by inflammation,

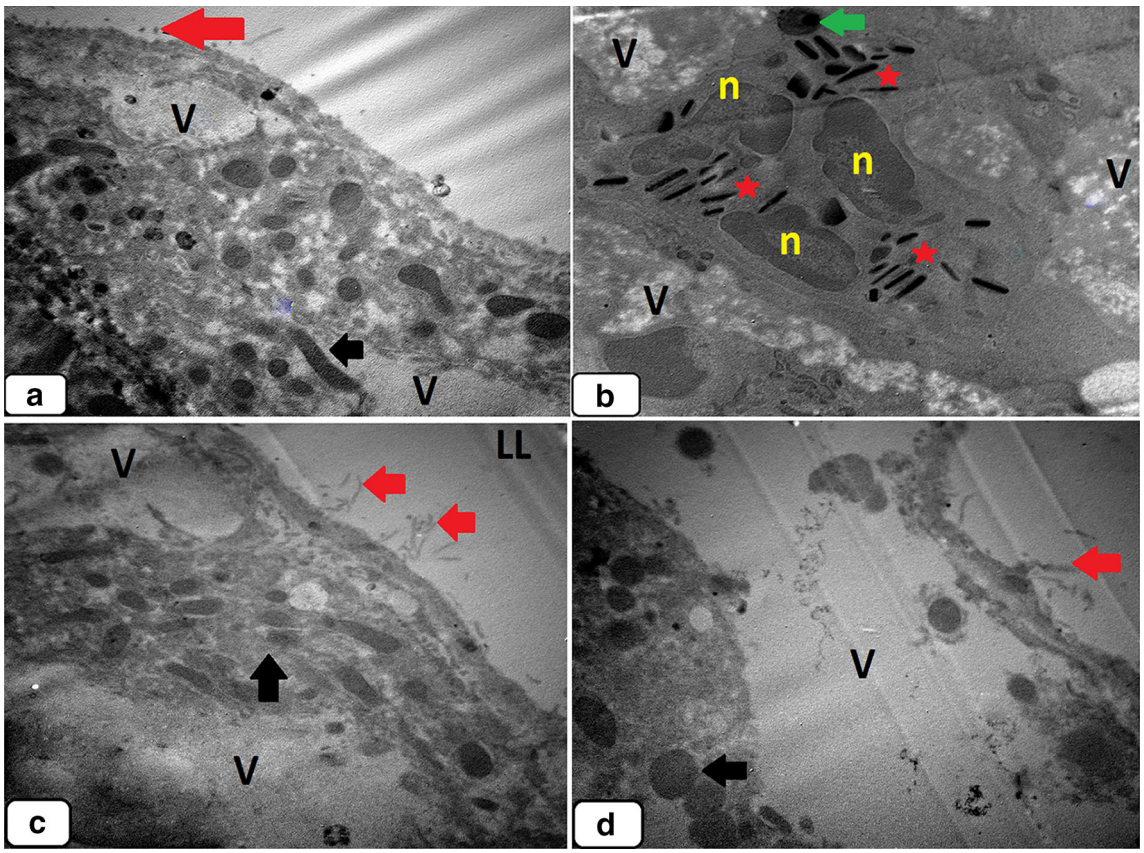

Fig. 7 Transmission electron micrograph of hydatid cysts **a** from nanosilver-treated mouse (GIV) showing destruction of the germinal layer and microtriches (red arrow). The cytoplasm is vacuolated (V) and shows distortion of the mitochondria (black arrows) with depletion of glycogen granules (×8000). **b** TEM micrograph of hydatid cysts from nanosilver-treated group (GIV) showing collections of Ag NPs appearing as electron-dense rods (red stars) inside the nucleus which is fragmented into pieces (n). The cytoplasm is vacuolated (V) and contains autophagosomes (green arrow) (×10,000). **c**, **d** TEM micrograph of hydatid cysts from ABZ-loaded NPs-treated group (GV) showing intense destruction of the germinal layer (red arrows) with separation from the laminated layer (LL), wide areas of vacuolated cytoplasm (V) with glycogen depletion and distorted mitochondria (black arrows) (×8000) (color figure online)

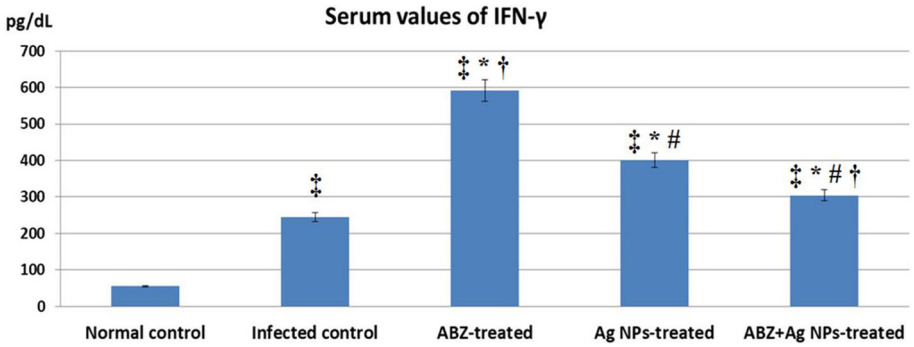

Fig. 8 Mean values of IFN-γ among the different studied groups. Data are expressed as mean ± SD, ‡ indicates significance ($P < 0.05$) of the value versus GI (normal control), * indicates significance versus GII (infected control), # indicates significance versus GIII (ABZ-treated) and † indicates significance versus GIV (Ag NPs-treated) by Kruskal–Wallis test followed by a post hoc test

necrosis, degenerative changes and may be accompanied by cholestasis (Ramachandran and Kakar 2009). Moreover, hepatotoxicity, neutropenia and nausea are common adverse effects of albendazole; therefore, ABZ is contraindicated with pregnancy and chronic liver diseases. Moreover, regular follow-up of leukocytes counts and liver

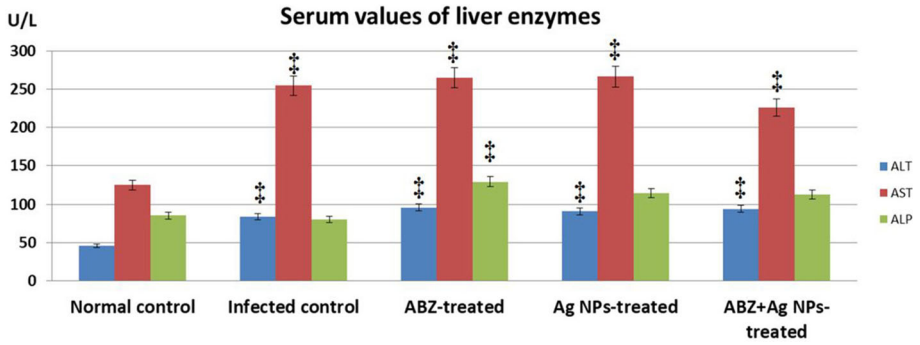

Fig. 9 Mean values of liver enzymes aspartate aminotransferase (AST), alanine aminotransferase (ALT) and alkaline phosphatase (ALP) among the studied groups. Data are expressed as mean ± SD, ‡ indicates significance ($P < 0.05$) of the value versus GI (normal control), * indicates significance versus GII (infected control), # indicates significance versus GIII (ABZ-treated) and † indicates significance versus GIV (Ag NPs-treated) Kruskal–Wallis test followed by a post hoc test

enzymes is recommended for all patients during ABZ treatment (Nunnari et al. 2012).

On the other hand, the safety and the anti-inflammatory effect of silver nanoparticles were reported previously when it was used against ulcerative colitis (Bhol and Schechter 2007). This safety was also reported by Loeschner et al. (2011). Similarly, Said et al. (2012) found that accumulated silver NPs in different organs was within the safe limits during their study on the efficacy of silver NPs against *Giardia lamblia* in experimental rats. Recently, the Food and Drug Administration (FDA) confirmed AgNPs as an effective agent against some bacterial and viral diseases (Burduşel et al. 2018).

Based on our findings and the previous literature, we assume that Ag NPs showed an anti-inflammatory effect besides an antiparasitic effect. The former is responsible for a protective effect against ABZ induced hepatotoxicity and the second is responsible for a synergistic antiparasitic action when it was combined with ABZ against CE; therefore, this combination showed the best results.

Concerning the serum values of IFN-γ in the present study, there were significant increases of the serum IFN-γ in all groups when compared with the normal control group (GI). The highest value was found in ABZ-treated group. Interestingly, there were significant reductions in serum IFN-γ when Ag NPs were used either alone or combined with ABZ. Moreover, the most significant decrease was in ABZ-loaded nanoparticles-treated group (GV). However these significant reductions, the values did not reach the normal values.

These findings are in agreement with Rigano et al. (1995) who found that after treatment or even the natural death of a cyst, TH2 response quickly drops and TH1 response becomes predominant. Additionally, Touil-Boukoffa et al. (1998) and Rostami-Rad et al. (2018) reported significant inductions of both TH1 and TH2 responses and elevation of TH1 cytokines levels, especially IFN-γ during *E. granulosus* infection. Moreover, Siracusano et al. (2008) found that the patients who responded to chemotherapy produced high amounts of IFN-γ.

In contrary, Rogan (1998) reported that during the late stage of experimental infection with *E. granulosus,* TH2 response dominates with elevated IL-10 and reduced IFN-γ. However, they detected high levels of IFN-γ in mice where cysts died after implantation, whereas low levels of IFN-γ were measured in mice harbouring live cysts. Accordingly, this is also consistent with our results as we assume that the different treatments resulted in the killing of the cysts, the release of *E. granulosus* antigens, stimulation of TH1 immune response and increase of IFN-γ production and the reduction of the elevated values towards the normal level seems to be dependent on the efficacy of the treatment. We also assume that the anti-inflammatory effect of Ag-NPs may be responsible for the most significant reduction of the IFN-γ toward the normal values when it was combined with ABZ although this combination showed the most significant antiparasitic effect against hydatid cysts.

Conclusion

The results of this study demonstrated that ABZ-loaded nanoparticles showed the best drug efficacy on experimental echinococcosis when it was compared with free nanosilver or ABZ treatments. ABZ-loaded on nanoparticles showed significant reductions of hydatid cyst size, weight and granuloma size with minimal histopathological effects on the liver tissues. Therefore, it could be considered as a new potential therapeutic option against *E. granulosus* infection; however, further studies should be done to evaluate this treatment from other aspects.

Acknowledgements The authors would acknowledge Prof. Ibrahim Shalash, the professor of Parasitology and Immunology at Theodor Bilharz Research Institute for his help in preparation of the nanoparticles.

Author's Contribution EVNB and SSS put the idea of the study. All authors prepared the research protocol and the study design. SSS isolated *E. granulosus* protoscoleces from hydatid cysts, carried out the experimental infection in mice, administrated the therapeutic doses, follow up of the mice, the parasitological study and tissue sampling. SSS and MAG performed mice sacrificing and collected the blood samples from mice, separated sera and carried out the measurement of liver enzymes and serum IFN-γ. ASEDM examined the stained liver sections and interpreted the histopathological results. SSS and EVNB interpreted the transmission electron microscopy results. SSS collected and tabulated the data while NEN, AES, NMH and EVNB participated in analysis and interpretation of the data. EVNB prepared and wrote the manuscript. All authors had read and approved the final manuscript.

Compliance with ethical standards

Conflict of interest Authors declare that there is no conflict of interest regarding the publication of this paper.

References

Ahmadnia S, Moazeni M, Mohammadi-Samani S, Oryan A (2013) In vivo evaluation of the efficacy of albendazole sulfoxide and albendazole sulfoxide loaded solid lipid nanoparticles against hydatid cyst. Exp Parasitol 135(2):314–319

Al-Kuraishi AH (2009) Histopathological changes of experimental hydatidosis in liver and spleen of albino mice: age and sex effect. J Fac Med 51(4):423–428

Amri M, Ait-Aissa S, Belguendouz H, Mezioug D, Touil-Boukoffa C (2007) In vitro antihydatic action of IFN-γ is dependent on the nitric oxide pathway. J Interferon Cytokine Res 27(9):781–787

Beigh AB, Darzi MM, Bashir S, Shah A, Shah SA (2017) Gross and histopathological alterations associated with cystic echinococcosis in small ruminants. J Parasit Dis 41(4):1028–1033

Bhol KC, Schechter PJ (2007) Effects of nanocrystalline silver (NPI 32101) in a rat model of ulcerative colitis. Dig Dis Sci 52(10):2732–2742

Burduşel AC, Gherasim O, Grumezescu AM, Mogoantă L, Ficai A, Andronescu E (2018) Biomedical applications of silver nanoparticles: an up-to-date overview. Nanomaterials 8(9):681

Drury RA, Wallington EA (1980) Carleton's histopathological techniques, 5th edn. Oxford University Press, Oxford, pp 129–130

Elissondo M, Dopchiz M, Ceballos L, Alvarez L, Bruni SS, Lanusse C, Denegri G (2006) In vitro effects of flubendazole on *Echinococcus granulosus* protoscoleces. Parasitol Res 98(4):317–323

Elissondo MC, Bermudez JM, Ullio Gamboa GV, Pensel PE, Cid AG, Juarez MM, Allemandi DA, Palma SD (2013) Hydatid disease: current status of chemotherapy and drug delivery systems. Curr Drug Ther 8(3):197–205

Farhadi M, Haniloo A, Rostamizadeh K, Faghihzadeh S (2018) Efficiency of flubendazole-loaded mPEG-PCL nanoparticles: a promising formulation against the protoscoleces and cysts of *Echinococcus granulosus*. Acta Trop 187:190–200

Grosso G, Gruttadauria S, Biondi A, Marventano S, Mistretta A (2012) Worldwide epidemiology of liver hydatidosis including the Mediterranean area. World J Gastroenterol 18(13):1425

Higuita NIA, Brunetti E, McCloskey C (2016) Cystic echinococcosis. J Clin Microbiol 54(3):518–523

Horton J (2018) Echinococcosis and albendazole: a case for suitable treatment. Am J Trop Med Hyg 99(4):811–812

Jelowdar A, Rafiei A, Abbaspour MR, Rashidi I, Rahdar M (2017) Efficacy of combined albendazol and praziquntel and their loaded solid lipid nanoparticles components in chemoprophylaxis of experimental hydatidosis. Asian Pac J Trop Biomed 7(6):549–554

Kandeel A, Ahmed ES, Helmy H, El Setouhy M, Craig PS, Ramzy RM (2004) A retrospective hospital study of human cystic echinococcosis in Egypt. East Mediterr Health J 10(3):349–357

Küster T, Stadelmann B, Aeschbacher D, Hemphill A (2014) Activities of fenbendazole in comparison with albendazole against *Echinococcus multilocularis* metacestodes in vitro and in a murine infection model. Int J Antimicrob Agents 43(4):335–342

Liang W, Wang XC, Wu XW, Zhang SJ, Sun H, Ma X, Peng XY (2014) Efficacy of albendazole chitosan microspheres against *Echinococcus granulosus* infection in mice. Chin J Parasitol Parasit Dis 32(3):188–192

Liang J, Li R, He Y, Ling C, Wang Q, Huang Y, Qin J, Lu W, Wang J (2018) A novel tumor-targeting treatment strategy uses energy restriction via co-delivery of albendazole and nanosilver. Nano Res 11(9):4507–4523

Loeschner K, Hadrup N, Qvortrup K, Larsen A, Gao X, Vogel U, Mortensen A, Lam HR, Larsen EH (2011) Distribution of silver in rats following 28 days of repeated oral exposure to silver nanoparticles or silver acetate. Part Fibre Toxicol 8(1):18

Luo Y, Zhang G, Liu X, Yuan M, Gao Q, Gao H, Ke L, Zhang X, Shi Y, Ma X, Zhang L (2018) Therapeutic and immunoregulatory effects of water-soluble alkaloids E2-a from *Sophora moorcroftiana* seeds as a novel potential agent against echinococcosis in experimentally protoscolex-infected mice. Vet Res 49(1):100

McManus DP, Gray DJ, Zhang W, Yang Y (2012) Diagnosis, treatment, and management of echinococcosis. BMJ 344:e3866

Moro P, Schantz PM (2009) Echinococcosis: a review. Int J Infect Dis 13(2):125–133

Noorani L, Stenzel M, Liang R, Pourgholami MH, Morris DL (2015) Albumin nanoparticles increase the anticancer efficacy of albendazole in ovarian cancer xenograft model. J Nanobiotechnol 13(1):25

Nunnari G, Pinzone MR, Gruttadauria S, Celesia BM, Madeddu G, Malaguarnera G, Pavone P, Cappellani A, Cacopardo B (2012) Hepatic echinococcosis: clinical and therapeutic aspects. World J Gastroenterol 13:1448

Palomares F, Palencia G, Ambrosio JR, Ortiz A, Jung-Cook H (2006) Evaluation of the efficacy of albendazole sulphoxide and praziquantel in combination on *Taenia crassiceps* cysts: in vitro studies. J Antimicrob Chemother 57(3):482–488

Pensel PE, Gamboa GU, Fabbri J, Ceballos L, Bruni SS, Alvarez LI, Allemandi D, Benoit JP, Palma SD, Elissondo MC (2015) Cystic echinococcosis therapy: albendazole-loaded lipid nanocapsules enhance the oral bioavailability and efficacy in experimentally infected mice. Acta Trop 152:185–194

Pensel P, Paredes A, Albani CM, Allemandi D, Bruni SS, Palma SD, Elissondo MC (2018) Albendazole nanocrystals in experimental alveolar echinococcosis: enhanced chemoprophylactic and clinical efficacy in infected mice. Vet Parasitol 251:78–84

Rahimi MT, Ahmadpour E, Esboei BR, Spotin A, Koshki MHK, Alizadeh A, Honary S, Barabadi H, Mohammadi MA (2015) Scolicidal activity of biosynthesized silver nanoparticles against *Echinococcus granulosus* protoscolices. Int J Surg 19:128–133

Rai M, Ingle AP, Paralikar P, Gupta I, Medici S, Santos CA (2017) Recent advances in use of silver nanoparticles as antimalarial agents. Int J Pharm 526(1–2):254–270

Ramachandran R, Kakar S (2009) Histological patterns in drug-induced liver disease. J Clin Pathol 62(6):481–492

Rigano R, Profumo E, Ioppolo S, Notargiacomo S, Ortona E, Teggi A, Siracusano A (1995) Immunological markers indicating the effectiveness of pharmacological treatment in human hydatid disease. Clin Exp Immunol 102(2):281–285

Rogan MT (1998) T-cell activity associated with secondary infections and implanted cysts of *Echinococcus granulosus* in BALB/c mice. Parasite Immunol 20(11):527–533

Rostami-Rad S, Jafari R, Yousofi-Darani H (2018) Th1/Th2-type cytokine profile in C57 black mice inoculated with live *Echinococcus granulosus* protoscolices. J Infect Public Health 11(6):834–839

Said DE, Elsamad LM, Gohar YM (2012) Validity of silver, chitosan, and curcumin nanoparticles as anti-*Giardia* agents. Parasitol Res 111(2):545–554

Shanmugasundaram T, Radhakrishnan M, Gopikrishnan V, Kadirvelu K, Balagurunathan R (2017) Biocompatible silver, gold and silver/gold alloy nanoparticles for enhanced cancer therapy: in vitro and in vivo perspectives. Nanoscale 9(43):16773–16790

Singh BB, Sharma JK, Tuli A, Sharma R, Bal MS, Aulakh RS, Gill JPS (2014) Prevalence and morphological characterisation of *Echinococcus granulosus* from north India. J Parasit Dis 38(1):36–40

Siracusano A, Riganò R, Ortona E, Profumo E, Margutti P, Buttari B, Delunardo F, Teggi A (2008) Immunomodulatory mechanisms during *Echinococcus granulosus* infection. Exp Parasitol 119(4):483–489

Solcan C, Solcan G, Ioniţă M, Hristescu DV, Mitrea IL (2010) Histological aspects of cystic echinococcosis in goats. Sci Parasitol 11(4):191–198

Solomon SD, Bahadory M, Jeyarajasingam AV, Rutkowsky SA, Boritz C, Mulfinger L (2007) Synthesis and study of silver nanoparticles. J Chem Edu 84(2):322–325

Soltani S, Rafiei A, Ramezani Z, Abbaspour MR, Jelowdar A, Kahvaz MS (2017) Evaluation of the hydatid cyst membrane permeability of albendazole and albendazole sulfoxide-loaded solid lipid nanoparticles. Jundishapur J Nat Pharm Prod 12(2):e34723

Stojkovic M, Zwahlen M, Teggi A, Vutova K, Cretu CM, Virdone R, Nicolaidou P, Cobanoglu N, Junghanss T (2009) Treatment response of cystic echinococcosis to benzimidazoles: a systematic review. PLoS Negl Trop Dis 3(9):e524

Touil-Boukoffa C, Bauvois B, Sancéau J, Hamrioui B, Wietzerbin J (1998) Production of nitric oxide (NO) in human hydatidosis: relationship between nitrite production and interferon-γ levels. Biochimie 80(8–9):739–744

Urrea-Paris MA, Moreno MJ, Casado N, Rodriguez-Caabeiro F (2002) Relationship between the efficacy of praziquantel treatment and the cystic differentiation in vivo of *Echinococcus granulosus* metacestode. Parasitol Res 88(1):26–31

Wang W, Li J, Yao J, Wang T, Li S, Zheng X, Duan L, Zhang W (2017) In vitro and in vivo efficacies of novel carbazole aminoalcohols in the treatment of cystic echinococcosis. J Antimicrob Chemother 72(11):3122–3130